Acta Societatis Botanicorum Poloniae

Authors' Contributions
WW and YC conceived the research, designed the experiments, and analyzed the data; WW, GZ, SW, HW, and TZ performed the research; WW wrote the paper

Competing Interests
No competing interests have been declared.

ORIGINAL RESEARCH PAPER in GENETICS, CELLULAR AND MOLECULAR BIOLOGY

Revealing the Core Transcriptome Modulating Plant Growth Phase in *Arabidopsis thaliana* by RNA Sequencing and Coexpression Analysis of the *fhy3 far1* Mutant

Wanqing Wang[1], Guoqiang Zhao[1], Shuang Wu[1], Wei Hua[1], Ting Zhang[1], Roger Ruan[2], Yanling Cheng ⬤[1,2*]

[1] Beijing Key Laboratory of Biomass Waste Resource Utilization, Biochemical Engineering College, Beijing Union University, Beijing, 100023, China
[2] Department of Bioproducts and Biosystem Engineering, University of Minnesota, Saint Paul, 55108, MN, United States

*To whom correspondence should be addressed. Email: cheng1012cn@aliyun.com

Abstract

Plants must continually calibrate their growth in response to the environment throughout their whole life cycle. Revealing the regularity of plant early growth and development is of great significance to plant genetic modification. It was previously demonstrated that loss of two key light signaling transcription factors, FHY3 and FAR1, can cause a stunted stature in the plant adult stage, and numerous defense response genes can be continuously activated. In this study, we performed a time-course transcriptome analysis of the early 4 weeks of leaf samples from wild plants and their *fhy3* and *far1* transcription factors. By comparative transcriptome analysis, we found that during the early 4 weeks of plant growth, plants primarily promoted morphogenesis by organizing their microtubules in the second week. In the third week, plants began to trigger large-scale defense responses to resist various external stresses. In the fourth week, increased photosynthetic efficiency promoted rapid biomass accumulation. Weighted gene coexpression network analysis of FHY3 and FAR1 revealed that the two light signaling transcription factors may be originally involved in the regulation of genes during embryonic development, and in the later growth stage, they might regulate gene expression of some defense-related genes to balance plant growth and immunity. Remarkably, our yeast two-hybrid and bimolecular fluorescence complementation experiments showed that FAR1 interacts with the immune signaling factor EDS1. Taken together, this study demonstrates the major biological processes occurring during the early 4 weeks of plant growth. The light signaling transcription factors, FHY3 and FAR1, may integrate light signals with immune signals to widely regulate plant growth by directly interacting with EDS1.

Keywords

weekly transcriptome analysis; plant development; different expression genes (DEGs); immune response

1. Introduction

As sessile organisms, plants must shape their growth and development in a time-dependent manner to survive a complex and changing environment. Plants perceive and integrate internal (e.g., circadian clock) and external signals (e.g., light and temperature) to adjust their self-development. In this process, large numbers of components, from genes and molecules to cells and tissues, interact at various scales.

To reveal details of the molecular machinery, many molecular analyses have been performed on the different plant stages from seed germination to leaf expansion to flowering. Recently, an emerging approach to monitor these elements in large numbers is the statistical analysis of spatial and temporal transcriptome data, a method that allows one to follow thousands of genes simultaneously. This can yield new insights into the underlying biological mechanisms of plant development.

Light is the most important environmental signal that influences plant growth and development. Higher plants have evolved a wide range of photoreceptors to sense information about the light in their environment. Among these photoreceptors, red light and far red light-absorbing phytochromes (phys) are the best characterized (Neff et al., 2000; Whitelam et al., 1993). Far-red elongated hypocotyl 3 (FHY3) and far-red-impaired response (FAR1) function as positive regulators and initiate phyA signaling by directly activating transcription of the downstream targets *FAR-RED ELONGATED HYPOCOTYL1 (FHY1)* and *FHY1-LIKE* (Hudson et al., 1999; Lin et al., 2007; Wang & Deng, 2002). Recent studies have demonstrated that FHY3 and FAR1 play multiple roles in plant growth and development, such as in photomorphogenesis (Wang & Deng, 2002), chloroplast division (Ouyang et al., 2011), chlorophyll biosynthesis (Tang et al., 2012), circadian clock (Li et al., 2011), abscisic acid responses (Tang et al., 2013), and plant immunity (Wang et al., 2016). These functions indicate that FHY3 and FAR1 are crucial for plant growth and development. Our previous report showed that the adult *fhy3 far1* mutant had slow, stunted growth, and displayed severe cell death under a long-day condition; this phenotype became even more severe under a short-day condition (Wang et al., 2016). Overexpression of the chlorophyll biosynthesis gene (*HEMB1*), salicylic acid (SA) metabolism and signal transduction-related genes (*NahG*, *PAD4*, *SID2*, and *EDS1*), and *myo*-inositol 1-phosphate synthase (*MIPS1*) could rescue these phenotypes in the *fhy3 far1* mutant (Ma et al., 2016; Tang et al., 2012; Wang et al., 2016). In addition, chromatin immunoprecipitation-sequencing (ChIP-seq) studies have shown that FHY3 has over 1,000 putative direct targets in *Arabidopsis*, suggesting that FHY3 might have broader functions in plant growth and development (Ouyang et al., 2011). However, when and why FHY3/FAR1 act as either activators or repressors in various developmental stages are still unknown.

RNA-seq is an effective method to analyze time-course gene expression and to obtain system-wide information about gene transcription and regulation. Recently, a high temporal-resolution investigation of maize seed transcriptomes separated the early endosperm dynamic transcriptome into four distinct groups corresponding to four developmental stages and unraveled the genetic control of early seed development (Yi et al., 2019). Using coexpression analysis, the core conserved stress-responsive genes (CARG) were discovered as involved in the response to multiple abiotic stresses in sesame species (Dossa et al., 2019). Through the weekly transcriptome analysis of *Arabidopsis halleri* for 2 years, seasonal transcriptomic dynamics were revealed, and a large number of seasonal genetic oscillations were defined. This was the first time molecular studies in the lab were combined with ecological studies in natural environments (Nagano et al., 2019).

2. Material and Methods

2.1. Preparation of Plant Material

Plant materials used in this study include the double mutant *fhy3 far1* (Lin et al., 2007; Wang & Deng, 2002) and wild type Nossen (NO). To avoid germination inconsistency results from seed material at different maturity levels, all seeds were surface sterilized and sown onto the MS plates containing 0.5% sucrose and 0.8% agar. After incubation for three days at 4 °C, seeds were transferred to the growth room with 60% humidity, and were cultured in a 16/8 hr (light/dark) photoperiod at 22 °C for 7 days. Then, the in-dish-grown 7-day-old seedlings were transferred into soil:vermiculite (3:1) mixture and were maintained under identical growth conditions with regular watering.

2.2. NBT and DAB Staining

For nitroblue tetrazolium (NBT) and 3,3′-diaminobenzidine (DAB) staining, leaves were separately submerged in staining solution (NBT staining solution: 1 mg mL^{-1} NBT, 0.1 mg mL^{-1} NaN$_3$, 10 mM potassium phosphate, pH 7.8; DAB staining solution: 0.1 mg mL^{-1} DAB, 50 mM Tris-acetate buffer pH 5.0) and stained overnight. The staining solution was replaced with a destaining solution (ethanol/glacial acetic acid/glycerol; 3:1:1) and was boiled for 10 min. After staining, all samples were photographed using a dissecting microscope.

2.3. Electrolyte Leakage Measurement

An electrolyte leakage assay was performed using a method described by Chen et al. (2013). Leaves were submerged in 5 mL of distilled water for 48 hr. The conductivity of the solutions was measured with a conductivity meter at regular intervals. Three biological replicates were set up for each of the measurement intervals. Statistical analysis was performed using the Student's t test.

2.4. Transcriptome Sequencing

For the transcriptome samples, plant samples (*fhy3 far1* mutant and NO wild type plants) were collected at four developmental stages: at 1-week-old cotyledons and at 2, 3, 4-week-old rosette leaves. Three independent biological replicates were set up for each genotype at the four given time points. We first randomly selected the 1-week-old seedlings of *fhy3 far1* and NO in the culture dish (about 20 seedlings for each sample). Then, the cotyledon sample was collected by manual dissection, snap-frozen in liquid nitrogen, and stored at −80 °C before processing. For the rosette leaf sample, each sample was obtained by pooling leaves from at least three plants. Specifically, for each 2-week-old sample, we randomly selected five plants in good growth status and collected the two largest true leaves from each plant. For the older samples, we selected three plants and then collected one larger true leaf at the same position from each plant.

Total RNA was isolated using the RNA Pure Plant Kit (Tiangen). RNA-seq libraries were constructed according to the manufacturer's protocol of the NEBNext Ultra RNA Library Prep Kit. The library was created using an Illumina HiSeq 2000 sequencing system.

2.5. RNA-Seq Data Analysis

Differentially expressed genes were screened by DESeq2 software (log2 fold change ≥ 1). The Blast2GO and ClusterProfiler programs were used to determine gene ontology (GO) and Kyoto Encyclopedia of Gene and Genomes (KEGG) functional enrichment, and q values less than 0.05 were considered as significant enrichment.

2.6. RNA Extraction and Quantitative RT-PCR

Plant total RNA was extracted using an RNA extraction kit (Tiangen), and first-strand cDNA was synthesized by reverse transcriptase (Invitrogen). Real-time PCR was performed according to the manufacturer's protocol of the SYBR Premix ExTaq Kit (Takara). All primers used are listed in Table S1. Three biological replicates were performed for each sample, and expression levels were normalized against those of *UBQ* controls.

2.7. Coexpression Analysis

For the weighted gene coexpression gene analysis, genes with a Pearson correlation coefficient (r) greater than 0.9 were considered to be significantly coexpressed genes with FHY3 and FAR1. The coexpression network was built using the Perl script, and data correlation and visualization were performed using the Cytoscape ver. 3.4.10 program (Smoot et al., 2011).

2.8. Plasmid Construction

To obtain the open reading frames of *FAR1*, *EDS1*, *PAD4*, and *SAG101*, the first-strand cDNA was reverse transcribed from total RNA extracted from Col WT seedlings using oligo $(dT)_{18}$ primer and high-fidelity FastPfu DNA Polymerase (TransGen). Fragments were cloned into the pEASY-Blunt vector (TransGen), resulting in pEASY-FAR1/EDS1/PAD4/SAG101 constructs, respectively. It should be noted that the translational stop codon in these genes was deleted to facilitate follow-up cloning. The primers are listed in Table S1, and all clones were validated by sequencing.

To construct vectors for the yeast two-hybrid assay, pEASY-PAD4 was digested with *Eco*RI and *Bam*HI, and the *PAD4* fragment was inserted into the pLexA vector (Clontech) cut by *Eco*RI and *Bam*HI to give rise to pLexA-PAD4. The pEASY-EDS1 plasmid was cut with *Mfe*I and *Xho*I, and pEASY-SAG101 was digested with *Mfe*I and *Sal*I, and the corresponding fragments were ligated into the *Eco*RI/*Xho*I sites of pLexA, producing pLexA-EDS1 and pLexA-SAG101, respectively. The yeast vectors pAD-FHY3 and pAD-FAR1 were described previously (Lin et al., 2007).

To prepare constructs for the BiFC assay, fragments from pEASY-FAR1 or pEASY-EDS1 cut with *Xba*I and *Xho*I were cloned into the pUC-SPYNE vector (Walter et al., 2004) digested with *Xba*I and *Xho*I, generating pYFP^N-FAR1 and pYFP^N-EDS1, respectively. The *EDS1* gene was released from pEASY-EDS1 cut with *Xba*I and *Xho*I and cloned into the *Xba*I– *Xho*I sites of the pUC-SPYCE vector, to generate pYFP^C-EDS1.

To construct *LUC* reporter genes driven by the *SID2* promoter, a 2-kb fragment upstream of the *SID2* ATG translation start code was PCR amplified with the SID2P1 and SID2P2 primers from Col genomic DNA. The PCR fragment was inserted into the pGEM-T Easy (Promega) vector to produce pGEM-SID2p. After sequencing confirmation, the *SID2* promoter was released from pGEM-SID2p cut with MfeI and SacI and ligated into the *Eco*RI–*Sac*I site of YY96 vector (Yamamoto et al., 1998) to produce SID2p:LUC.

2.9. Yeast Two-Hybrid Assay

Yeast two-hybrid analysis was performed according to the *Yeast protocols handbook* (2009). Briefly, the AD fusion plasmids were transformed into the Ym4271 strain, while LexA-fusion plasmids were transformed into EGY48 strain. After mating, transformants were grown on SD/Trp-Ura-His dropout plates containing X-gal for blue color development, from which the relative β-galactosidase activity was quantified.

2.10. BiFC Assay

For the BiFC assay in *Nicotiana benthamiana* leaves, *Agrobacterium tumefaciens* strain GV3101 containing the described plasmids was grown overnight in LB medium. The cultures were pelleted and resuspended in equal volumes of induction medium (10 mM MgCl$_2$, 10 mM MES pH 5.7, 0.2 g L^{-1} acetosyringone) for 3 hr at 28 °C. The p19 protein of the tomato bushy stunt virus was used to suppress gene silencing (Voinnet et al., 2003). The desired agrobacterium cultures were combined to an OD$_{600}$ ratio of 0.7:0.7:1 (YFP^N-fused plasmid:YFP^C-fused plasmid:p19 silencing plasmid) and were infiltrated into the leaves of 3-week-old *N. benthamiana*. Fluorescence was visualized in the epidermal cell layers of the leaves 2–3 days after infiltration using a confocal microscope (Olympus).

2.11. Luciferase Reporter Assay

For transient expression assays, *Agrobacterium* strains containing SID2p:LUC reporter plasmids, various effector constructs (Myc-FHY3, Myc-FAR1, or Myc-EDS1), 35S:GUS internal control and p19 silencing plasmids were mixed at a ratio of 0.7:0.7:0.3:1, and these were coinfiltrated into the abaxial surface of *N. benthamiana* leaves. Three days after infiltration, proteins from *N. benthamiana* leaves were extracted with the 1× Cell Culture Lysis Reagent (Promega). LUC and GUS activities were quantified as previously described (Tang et al., 2012). The relative reporter gene expression levels were expressed as LUC/GUS ratios.

3. Results

3.1. Loss of FHY3/FAR1 Stunts Plant Growth and Initiates Premature Cell Death

In our previous study, we noticed that the *fhy3 far1* mutant plant displayed a stunted stature in the adult stage (Wang et al., 2016). To further investigate how FHY3 and FAR1 regulate plant growth, we analyzed the phenotypes of the *fhy3 far1* mutant at different developmental stages. Aside from having an elongated hypocotyl, the *fhy3 far1* mutant did not differ much from the NO (Nossen) wild type during the first 2 weeks (Figure 1A). Remarkably, 3-week-old *fhy3 far1* grew slowly and had a retarded leaf area increase rate (Figure 1F). During week 4, the wild type grew rapidly, and its average leaf area quadrupled, reaching 5.9 cm². In comparison, the *fhy3 far1* mutant had significantly reduced vegetative growth, and its leaf area was less than one-tenth of the wild type. The leaves of the *fhy3 far1* mutant visibly developed necrotic lesions.
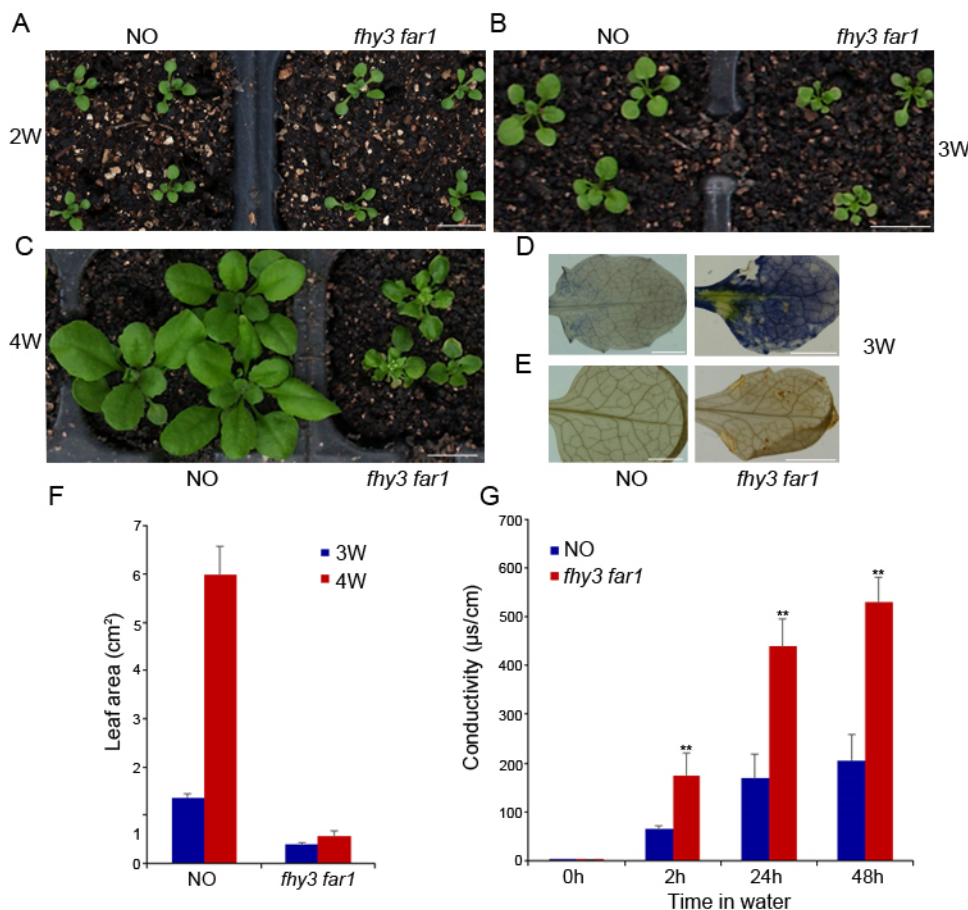
Figure 1 Phenotypic analysis of the *fhy3 far1* double mutant. (**A–C**) Morphology of the NO wild type (WT) and *fhy3 far1* plants grown on soil under long day (LD; 16 hr light / 8 hr dark) for 2–4 weeks. Bars: 1 cm. Nitroblue tetrazolium (NBT) (**D**) and 3,3′-diaminobenzidine (DAB) (**E**) staining of WT and *fhy3 far1* leaves grown under LD conditions for 3 weeks. Bars: 1 mm. (**F**) Areas of 3-week-old and 4-week-old leaves were measured using ImageJ software. Data are represented as mean ± *SD*; *n* = 9. (**G**) Electrolyte leakage of the double mutant and wild type. Three-week-old leaves were immersed in water, and electrolyte leakage was measured periodically. Asterisks denote statistically significant differences in electrolyte leakage compared with WT (*p* < 0.01, Student's *t* test). Similar results were obtained in three independent experiments.

When stained with 3,3′-diaminobenzidine (DAB) and nitroblue tetrazolium (NBT) (which indicates hydrogen peroxide and superoxide accumulation), the 3-week-old leaves of *fhy3 far1* were heavily stained, whereas those of the wild type were barely stained (Figure 1E,F). To determine whether photooxidative damage resulted in cell death in the *fhy3 far1* mutant, we analyzed the cell death-induced electrolyte leakage of the 3-week-old leaves. In agreement with the DAB and NBT staining

results, electrolyte leakage was significantly greater in *fhy3 far1* than in wild type (Figure 1G). Taken together, our results indicate that *FHY3* and *FAR1* play key roles in controlling plant growth especially during the early third week.

### 3.2. Weekly Dynamic of Transcriptomes in the Wild Type

In order to explore the possible molecular mechanism of plant growth and development, 24 leaf samples at four different developmental stages were collected and subjected to Illumina paired-end sequencing. After cleaning and filtering out low quality and ambiguous reads, 506 million clean reads containing 151 Gb of valid data were acquired (Table 1). The sequencing data were deposited in the National Center for Biotechnology Information (NCBI) database (accession number: SRP229410).

Table 1 Summary of the wild type and double mutant transcriptome data obtained by Illumina sequencing.

Sample	Raw reads (*n*)	Clean reads (*n*)	Q20 (%)	Q30 (%)	GC content (%)
W1-WT1	26,923,440	26,449,878	96.39	90.96	45.22
W1-WT2	19,968,581	19,303,569	96.31	90.72	44.85
W1-WT3	22,383,567	21,901,461	96.19	90.44	45.20
W1-M1	22,770,145	22,490,651	95.52	89.11	45.48
W1-M2	23,291,104	22,995,557	95.88	89.87	45.43
W1-M3	22,999,218	22,673,082	95.51	89.18	45.49
W2-WT1	23,796,028	23,508,457	96.14	90.38	45.35
W2-WT2	19,843,161	19,497,793	95.84	89.81	44.78
W2-WT3	19,977,547	19,437,941	95.82	89.76	44.19
W2-M1	22,579,272	22,255,754	95.56	88.99	43.77
W2-M2	21,543,657	20,412,505	96.91	91.51	44.66
W2-M3	20,223,672	20,014,132	96.42	90.91	44.58
W3-WT1	16,406,848	16,190,140	97.34	95.59	45.59
W3-WT2	22,811,865	22,499,706	97.38	95.94	45.27
W3-WT3	16,624,043	16,406,307	97.37	95.61	45.53
W3-M1	21,061,087	20,701,821	97.49	95.28	44.89
W3-M2	20,400,525	20,126,584	97.62	95.50	44.82
W3-M3	21,247,314	20,988,523	97.57	96.16	44.70
W4-WT1	19,355,011	18,889,955	96.14	90.37	45.77
W4-WT2	22,998,752	22,047,939	96.09	90.30	46.00
W4-WT3	21,755,411	21,238,281	96.04	90.16	45.84
W4-M1	22,681,243	22,308,943	95.75	89.63	44.39
W4-M2	22,591,592	22,309,718	96.08	90.26	44.39
W4-M3	22,358,130	22,067,189	96.20	90.49	44.38

To reveal the vital biological processes of the different growing stages, we first analyzed the weekly transcriptome dynamics of the wild type. Compared with the previous week, there were 1,741 upregulated genes and 3,050 downregulated genes (Figure 2). A total of 1,353 and 1,741 genes were induced in the third and fourth weeks, respectively, whereas 805 and 1,619 were repressed. Based on the analysis of the numbers of differentially expressed genes (DEGs), we found that the early-stage gene modification was highly dynamic, especially in 2-week-old leaf tissue, and that this transcriptome modulation would play a vital role in the subsequent growth and development of plants.

To gain further functional insights, DEGs were assigned to GO terms such as cellular component, molecular function, and biological process. Comparing GO annotations from genes in 2-week rosette leaves with those of 1-week cotyledons, we found that the 2-week upregulated genes were closely related to the dynamic arrangement of microtubules (MTs), These comparisons included cellular component (kinesin complex and microtubule), molecular function (microtubule motor activity and microtubule binding), and biological process (microtubule-based movement and
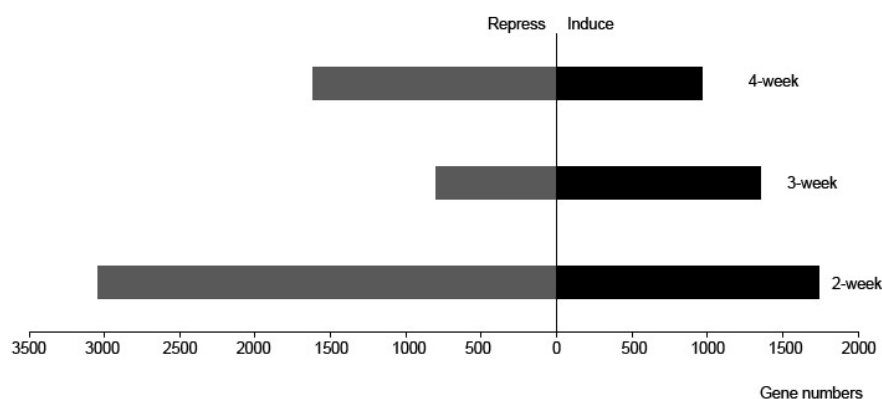
Figure 2 The number of differentially expressed genes (DEGs) in each week. Number of DEGs with a *q* value of <0.05 and a fold change of >2 in the 2, 3, and 4-week-old NO leaves.

microtubule cytoskeleton organization) (Figure 3A). The dynamic behavior of the MTs played a pivotal role in controlling cell growth and shape formation, and MT-associated proteins (MAPs) controlled MT dynamics, stability, and organization (Lloyd & Hussey, 2001; Sedbrook, 2004). The IQ67 DOMAIN (IQD) protein family is known as the largest and most important class of MAPs in plant development and in plant responses to the environment (Bürstenbinder et al., 2007; Liang et al., 2018). Here, we found that *IQD8*, *IQD21*, and *IQD25* displayed significantly increased expression in the 2-week leaf growth (Figure 4). *JAGGED*, a zinc finger transcription factor encoding a gene controlling anisotropic growth, was also induced in the second week stage (Schiessl et al., 2014). Moreover, DNA replication, chromatin binding, and translation categories were significantly overrepresented, and a larger number of nuclear- and ribosome-localized proteins were also enriched among the 2-week upregulated genes. This was consistent with the established *Arabidopsis* MAP proteome data (Hamada et al., 2013). In the MAP-enriched proteome database, proteins implicated in replication, transcription, and translation were highly enriched. Moreover, proteins involved in RNA transcription-related processes constituted 23.5%, proteins involved in DNA replication accounted for 5.0%, and proteins with roles in translation accounted for 5.7%. The second week is a critical period for plant growth, and in this period, plants initially differentiate the true leaf and conduct early leaf morphogenesis through cell proliferation and cell expansion. A similar transcriptional change was observed in the temporal transcriptome of maize seed development. Consistent with the active nuclear division and cell proliferation that occur at the coenocyte formation stage of the maize seed, functional categories of DNA replication, transcription factor activity, DNA binding, microtubule-based movement, microtubule motor activity, and nucleosome assembly were also overrepresented in its coexpression modules (Yi et al., 2019). Hence, tissue formation of different plant materials may have common mechanisms. In the second week, the wild type (NO) initially conducts early true leaf morphogenesis by activating DNA/RNA-related processes and microtubule arrangement. When examining the downregulated genes, the largest negative DEGs mainly belonged to oxidoreductase activity and plant stress-response which are often accompanied with higher redox activity (Figure S1). In addition, it should be noted that addition of sucrose in the MS medium would influence gene expression in 1-week-old seedlings. To avoid germination inconsistency resulting from seed materials at different maturity, all seeds were sown onto the MS plates containing 0.5% sucrose and were grown for 7 days. It is known that sucrose not only serves as a carbon skeleton supply but also acts as a signal molecule that regulates a variety of growth and developmental processes in plants. It has been reported that low concentrations (0.5%–1%) of sucrose promotes seed germination, primary root growth, and hypocotyl elongation at the earliest stages of plant growth (Singh et al., 2017). We compared the 1-week upregulated genes with sucrose-

responsive genes (Blasing et al., 2005) and found that 87 sucrose-induced genes were upregulated in the 1-week-old cotyledons grown in a dish compared to the 2-week-old leaves grown in soil (Appendix S1). This was consistent with the presentation of the functional category of sucrose metabolic processes among the 2-week downregulated genes (Figure S1).

It is often assumed that growth and defense are negatively correlated. Plants must efficiently allocate their resources between stress-response pathways and growth-promoting pathways to be successful during the developmental stage. Compared with the second week, a larger number of stress process-related genes were positively regulated in the third week (Figure 3B). These primarily included the following: oxidoreductase activity, iron homeostasis, and response to stress and defense. Enhanced cellular oxidation has an important function on the regulation of plant growth and stress responses (Considine & Foyer, 2014). Iron ions can exist in both the ferric and the ferrous forms and can function as a crucial redox catalyst in many cellular processes such as DNA replication, energy production, and plant immunity (Cassat & Skaar, 2013; Ganz & Nemeth, 2015; Luo et al., 1994). *MPK3* encodes a mitogen-activated protein kinase that is an important component of ROS signaling pathways (Mittler et al., 2011). The bHLH transcription factor FIT functions as the central regulator of the Strategy I iron-uptake response (Colangelo & Guerinot, 2004; Jakoby et al., 2004). As shown in Figure 4, the expression levels of *MPK3* and *FIT* were increased in the leaves during the third week. We compared the 3-week upregulated genes with genes responding to pathogen infection (Bartsch et al., 2006). We found that 225 pathogen-induced genes were represented in the upregulated group (Appendix S1). In addition, a total of 17 *R* genes, which code for proteins that recognize a specific pathogen effector, were induced in the third week stage. Consistently, transcript levels of *PR* genes (pathogenesis-related gene) including *PR1*, *PR4*, and *PR5* were also greatly upregulated. Together, these results indicate that the 3-week plant initially activates response signals to modify plant growth in response to changing environmental conditions. Subsequently, we analyzed the DEGs of 4-week leaves by comparing with the third week, and we found that upregulated DEGs were mainly assigned to photosynthesis (Figure 3C). These genes include those that encode major photosynthetic complexes of the LHCA and LHCB protein families, photosystem I/II subunits, and chlorophyll synthesis-related key enzymes (HEMA1, CHLH, GUN4, CAO, and PORA). Four of these, i.e., *LHCB1.1, HEMA1*, *CHLH*, and *PORA*, were selected and were confirmed to be induced in the fourth week stage by quantitative RT-PCR (qRT-PCR) analysis (Figure 4). Furthermore, the categories of oxidoreductase activity, response to auxin, and signal transduction were also significantly overrepresented among the 4-week upregulated genes. Intracellular redox interactions are important for developmental processes. Chloroplasts are powerful generators of redox signals through the core process of photosynthesis. The plant cell requires monitoring of chloroplast status to emit signals that regulate nuclear gene expression in a timely manner. Compared with the ROS transcriptional footprints (Willems et al., 2016), we found that 23 Genomes Uncoupled (GUN) retrograde signaling-related genes were represented in the 4-week upregulated genes, including two chlorophyll biosynthetic genes and 12 photosystem subunit genes (Appendix S1). Plants rely on photosynthesis to convert solar energy, carbon dioxide, and water into chemical energy and biomass. This increased photosynthetic efficiency contributes to rapid biomass accumulation, and this was consistent with the rapidly increased leaf area of the 4-week-old wild type.

3.3. Analysis of Differentially Expressed Genes (DEGs) in *fhy3 far1* Mutant

To further examine key biological processes in the various developmental stages, we conducted 4 weeks of transcriptome analysis of the growth retardation mutant *fhy3 far1*. Compared with NO, the number of DEGs in each developmental phase of the *fhy3 far1* mutant was significantly increased especially in the first 3 weeks (Figure 5). In the mutant, there were 2,139 upregulated genes and 3,132 downregulated genes in the 2-week samples, while in the 3-week leaves, 3,475 genes were upregulated and 2,335 ones were downregulated, respectively, compared with the previous week. Out of those upregulated genes, only 231 out of 2,139 (10%) and 385 of 3,475 (11%) showed similar expression patterns with the wild type. These results indicate that
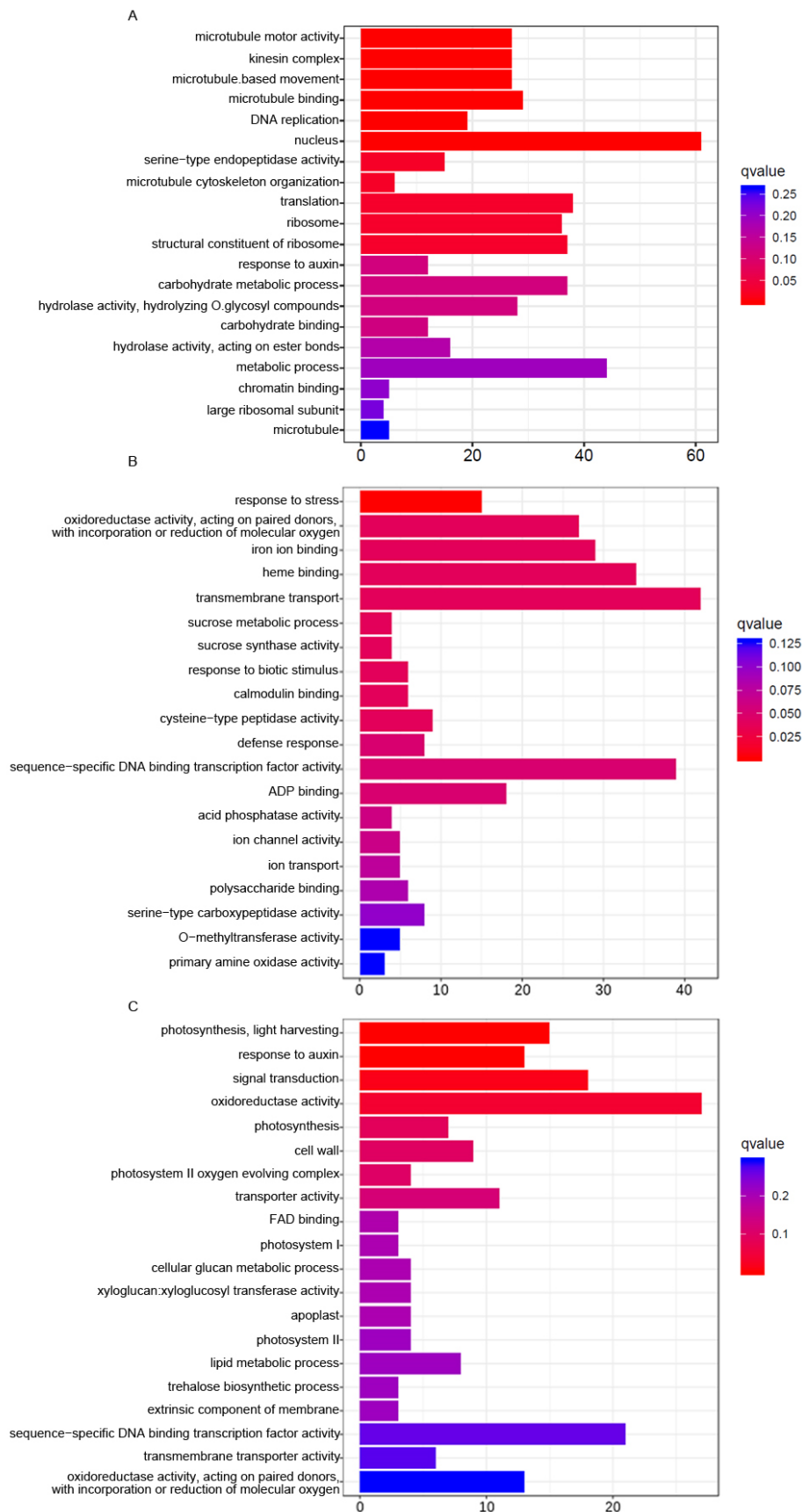
Figure 3 Enrichment of selected categories of GO biological processes in genes upregulated in 2 (**A**), 3 (**B**), and 4 (**C**) week NO leaves compared to the previous week. Functional annotation of upregulated genes into the biological process, cellular component, and molecular function categories within the gene ontology (GO) database.
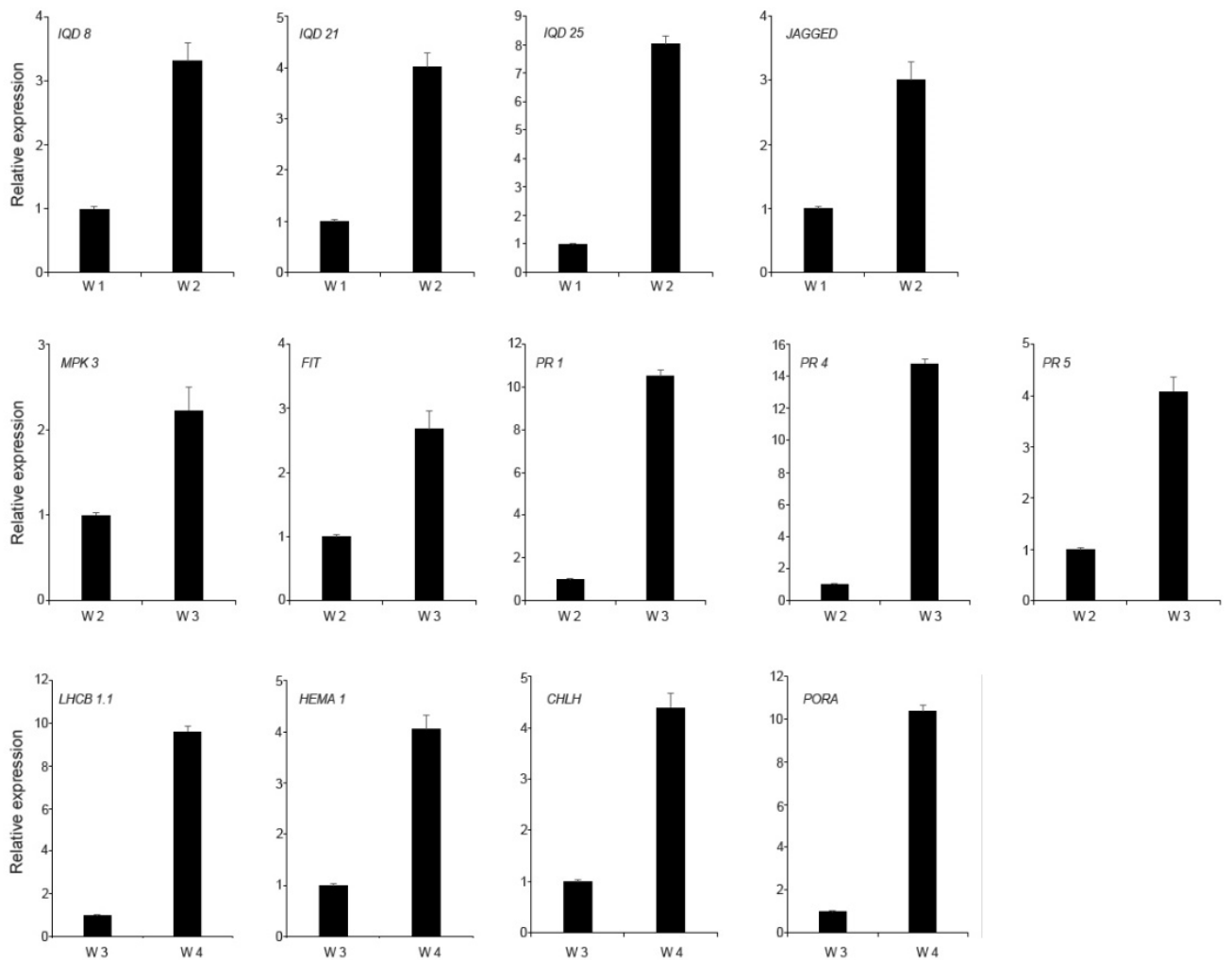
Figure 4 Validation of RNA sequencing results by real-time quantitative PCR. Relative expression of various genes determined by qRT-PCR in the NO wild type during different developmental stages. Relative expression was normalized to *UBQ1* levels. Bars indicate the *SD* of three biological replicates.

FHY3 and FAR1 play an important role in various plant developmental stages, especially during the first 3 weeks, and that the loss of FHY3 and FAR1 causes large-scale changes in transcriptome.

After classifying the DEGs under their GO terms, we found that *fhy3 far1* had the largest positive difference in DEGs under transmembrane transport activity in the second week, including drug transmembrane transport, ion transport, transferase activity, and channel activity (Figure S2). We also observed that the oxidoreductase activity also showed high activity in the second week. Together with the eukaryotic ortholog groups (KOG) analysis result, we found that defense responses were pretriggered in the second week (Figure S3), and those that induced transmembrane transport activity and oxidoreductase activity may partly contribute to the immune response. Comparing the genes responding to pathogen infection, we found that 530 pathogen-induced genes were represented in the 2-week upregulated group of *fhy3 far1* (Appendix S1). Unlike the wild type, early morphogenesis-related microtubules activity was also delayed to the third week in the mutant. Compared to gene expression in the second week, 132 MAPs-coding genes were found to be upregulated in the 3-week-old mutant (Appendix S1). It is known that both MT assembly and dynamics are assisted by the coordinated action of MAPs. Comparing DEGs of *fhy3 far1* and NO in various development stages also revealed that the number of DEGs in the second week was far greater than in the other stages and
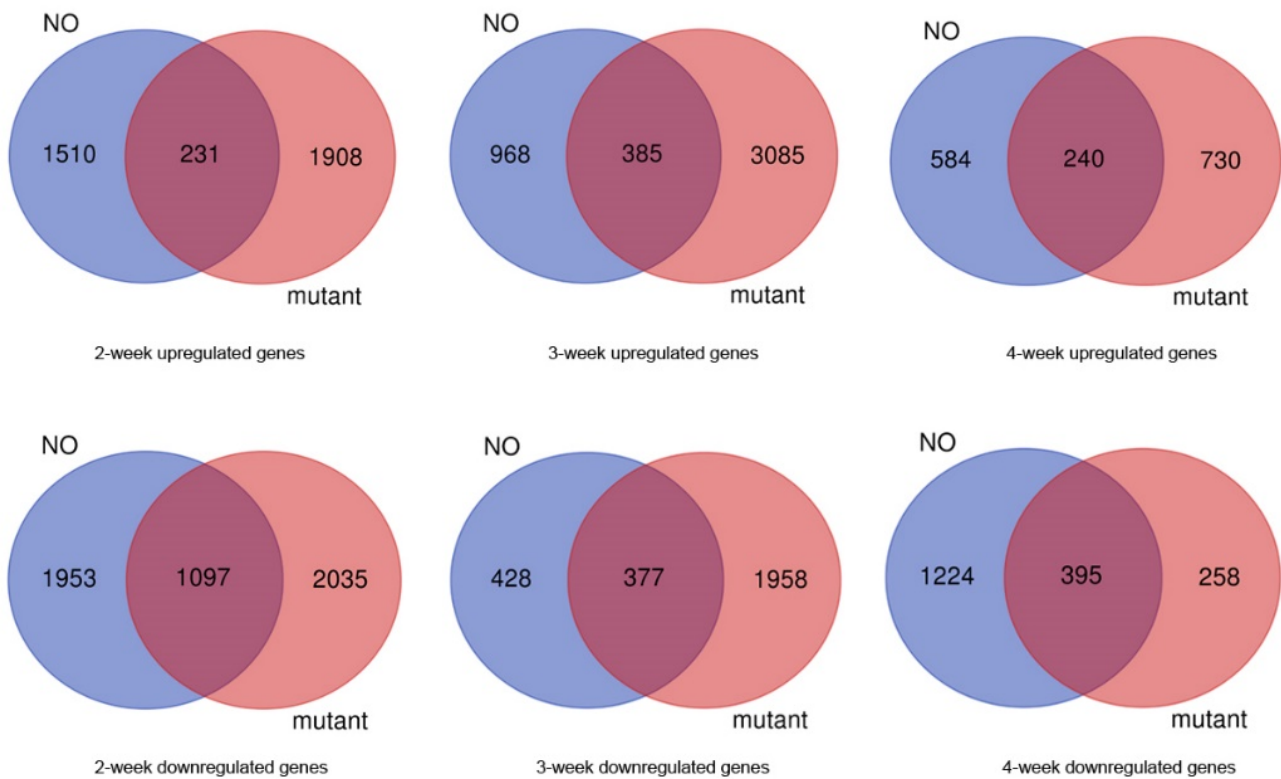
Figure 5 Transcriptome analysis of FHY3/FAR1-regulated genes. The Venn diagram shows the overlap of upregulated and downregulated genes in NO and *fhy3 far1* samples under various stages. The numbers in the circles indicate the number of genes changed in each week.

that many genes closely related to microtubule activity were indeed differentially expressed in this week (Figure 6B). These results suggest that FHY3 and FAR1 are two key transcriptional factors that positively regulate MT assembly and properly inhibit the hypersensitive response in the second week to ensure optimal plant growth. Loss of FHY3 and FAR1 led to the gradual appearance of the stunted stature and necrotic lesions in the third week. In addition, we found that the protein kinase activity and protein phosphorylation categories were also significantly overrepresented among the DEGs of *fhy3 far1* and NO. Protein phosphorylation is a dominant mechanism of information transfer in cells. Both the MT arrangement process and plant immunity response are accompanied by the phosphorylation of a large number of proteins. In the regulation of MT arrangement, MAPs and other regulators of MT dynamics are modified post-translationally through reversible phosphorylation to reorganize the microtubule cytoskeleton for environmental and developmental changes (Sasabe et al., 2006; Wasteneys & Ambrose, 2009). It is also known that mitogen-activated protein kinases (MAPKs) are important regulators of plant immunity. Compared to wild type, we observed that several MAPK-encoding genes (*MPK1*, *MPK2*, *MPK3*, *MPK7*, *MPK11*, and *MPK15*) and MAPK cascades (MKK4/MKK5-MPK3 and MKK1/MKK2-MPK4) that are involved in plant responses to biotic stress were activated in the 2-week-old mutant. Together, these data indicate that FHY3 and FAR1 play important regulatory functions in the key biological processes in the early developmental stages of the plant, and that the loss of these two transcription factors can cause large-scale changes in the transcriptome and disrupt cellular metabolism, finally resulting in stunted growth and an out-of-control defense response.

3.4. Identification of *FHY3/FAR1* Coexpressed Genes

To obtain more information about the regulatory function of the transcription factors FHY3/FAR1, coexpression analysis using the Cytoscape software was carried
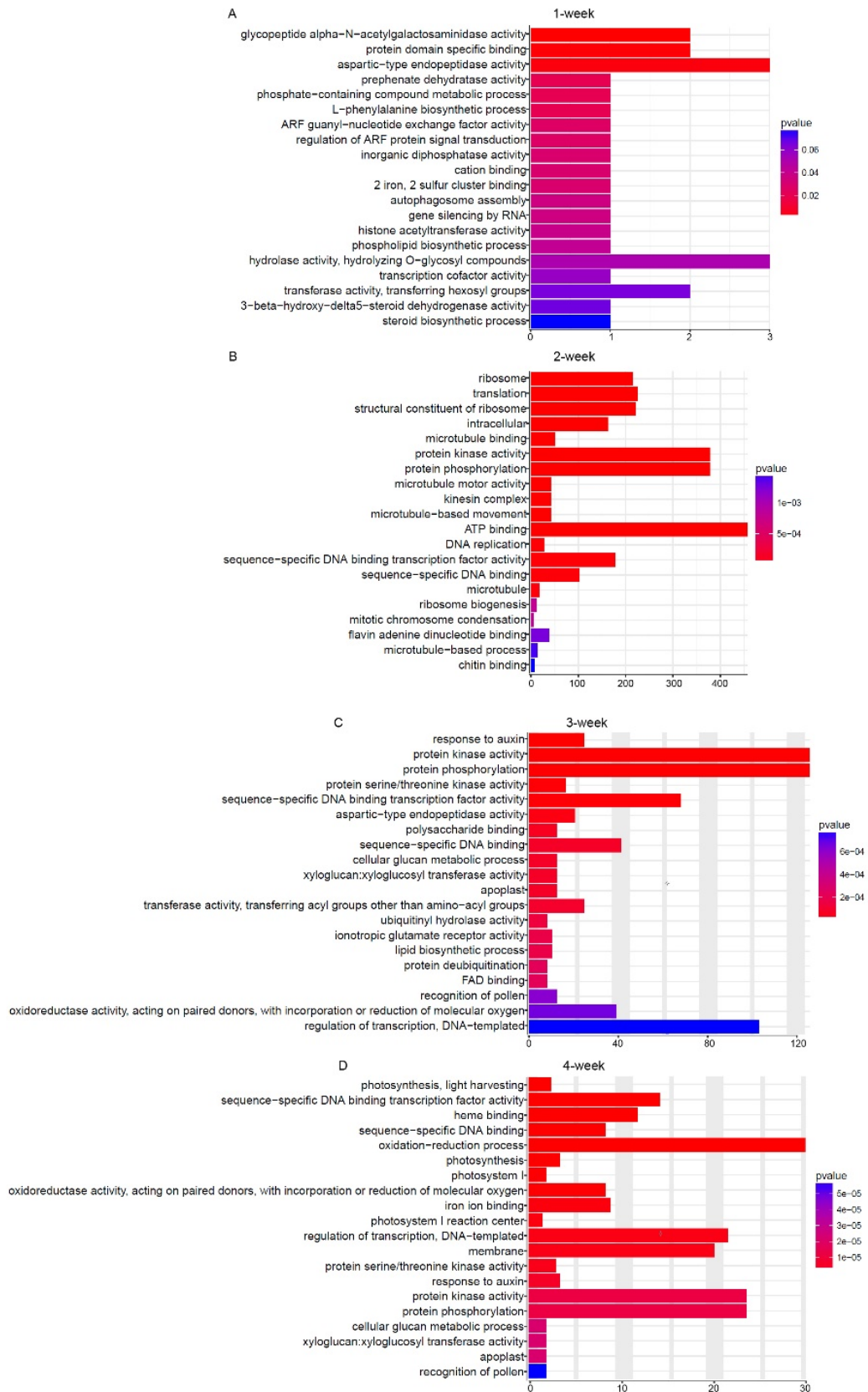
Figure 6 FHY3/FAR1 regulates genes with diverse functions. Enrichment of selected categories of GO biological processes in genes differentially expressed in *fhy3 far1* compared to the wild-type genome in 1 (**A**), 2 (**B**), 3 (**C**), and 4 (**D**) week. Functional annotation of those differentially expressed genes into the biological process, cellular component, and molecular function categories within the GO database.

out to determine specific genes that may be associated with the two genes. We identified a total of 40 genes that were coexpressed with *FHY3* and 81 genes that were coexpressed with *FAR1* during the early 4 weeks of growth (Figure 7). Among those genes, there were 19 genes with coexpression of both *FHY3* and *FAR1*. This indicates that FHY3 mostly works with its homolog FAR1 to exert regulatory function; moreover, we found that FAR1 seems to have a broader regulatory role. Then, we divided the coexpressed genes into different molecular clusters. As shown in Figure 7, red-labeled genes represent the 19 coexpressed genes of both *FHY3* and *FAR1*. Most interestingly, there were seven defense response genes (including two TIR-NBS-LRR *R* genes), two cell differentiation related genes, three hormonal biosynthesis regulation genes (*ABA3*, *KAO1*, and *WRKY46*), and four oxidoreductase activity genes that were coexpressed with *FHY3*. Consistent with previous studies, the *fhy3 far1* double mutant showed a lesion mimic phenotype, and a number of defense related genes were largely induced (Wang et al., 2016). These results indicate that FHY3 is involved in the defense response, likely by regulating the TIR-NBS-LRR-mediated genes. Another gene that deserves attention is *WRKY46*, a well conserved WRKY domain transcription factor that plays crucial roles in plant innate immunity as well as in abiotic stress responses (Ding et al., 2014; Götz et al., 2008; Hu et al., 2012). It has been reported that WRKY46 could regulate abscisic acid (ABA) signaling and auxin homeostasis to inhibit lateral root development under osmotic stress conditions (Ding et al., 2015). Similarly, FHY3 could modulate ABA signaling and SA signaling to regulate plant development and plant immunity (Tang et al., 2013; Wang et al., 2016).

Thus, we speculate that *FHY3* may associate with *WRKY46* to collectively regulate cellular hormone levels to control the growth and stress response processes. Going back to *FAR1*, we found that it has nine coexpressed genes which were specifically expressed at the embryonic stage, four defense response genes, and three iron homeostasis-related genes. Thus, we speculate that FAR1 may play an important role in the early development stage, and this may be through the regulation of redox homeostasis and inhibition of the early immune response to promote plant growth. Combined with the phenotype of *fhy3 far1* mutant, these data indicate that the two light signaling factors may be associated with the positive regulation of early embryonic development and in the later growth stage may negatively regulate expression of defense-related genes to balance plant growth and immunity.

FAR1 Physically Interacts With EDS1

Our previous study indicated that FHY3 and FAR1 negatively modulate plant immunity by regulating the NB-LRR-mediated SA signaling pathway to the defense response (Wang et al., 2016). Enhanced disease susceptibility1 (EDS1) is regarded as a central regulator of plant innate immunity, and it interacts with two sequence-related proteins, Phytoalexin deficient 4 (PAD4) and Senescence-associated gene 101 (SAG101), and operates upstream of pathogen-induced SA accumulation (Feys et al., 2001, 2005). To explore how the transcription factors FHY3/FAR1 participate in the regulation of immune signaling, we first focused on three nuclear localization immune signaling factors, EDS1, PAD4, and SAG101, which appear to travel between the nucleus and cytoplasm. The movement of these proteins is important for transcriptional reprogramming in disease resistance (Wiermer et al., 2007; Vlot et al., 2009). We attempted to test whether these proteins could interact with FHY3 and FAR1 in the nucleus. In a yeast two-hybrid assay, we found that a combination of LexA-EDS1 (EDS1 fused to the DNA-binding domain of LexA) and AD-FAR1 (FAR1 fused to the activation domain of B42) strongly activated *LacZ* reporter gene expression, indicating that EDS1 and FAR1 interact in yeast cells (Figure 8A,B). We also observed that FHY3 weakly interacted with EDS1; however, no interaction was observed between FHY3/FAR1 and PAD4 or SAG101 (Figure 8A). To test this notion in vivo, we carried out a bimolecular fluorescence complementation (BiFC) assay in *Nicotiana benthamiana* leaves via an *Agrobacterium*-mediated transient expression approach. As positive controls, YFP[N]-EDS1 (EDS1 fused to the N-terminus of yellow fluorescence protein) and EDS1-YFP[C] (EDS1 fused to the C-terminus of YFP) interacted and produced fluorescence signals in the nucleus and cytoplasm (Figure 8D). We observed that coexpression of YFP[N]-FAR1
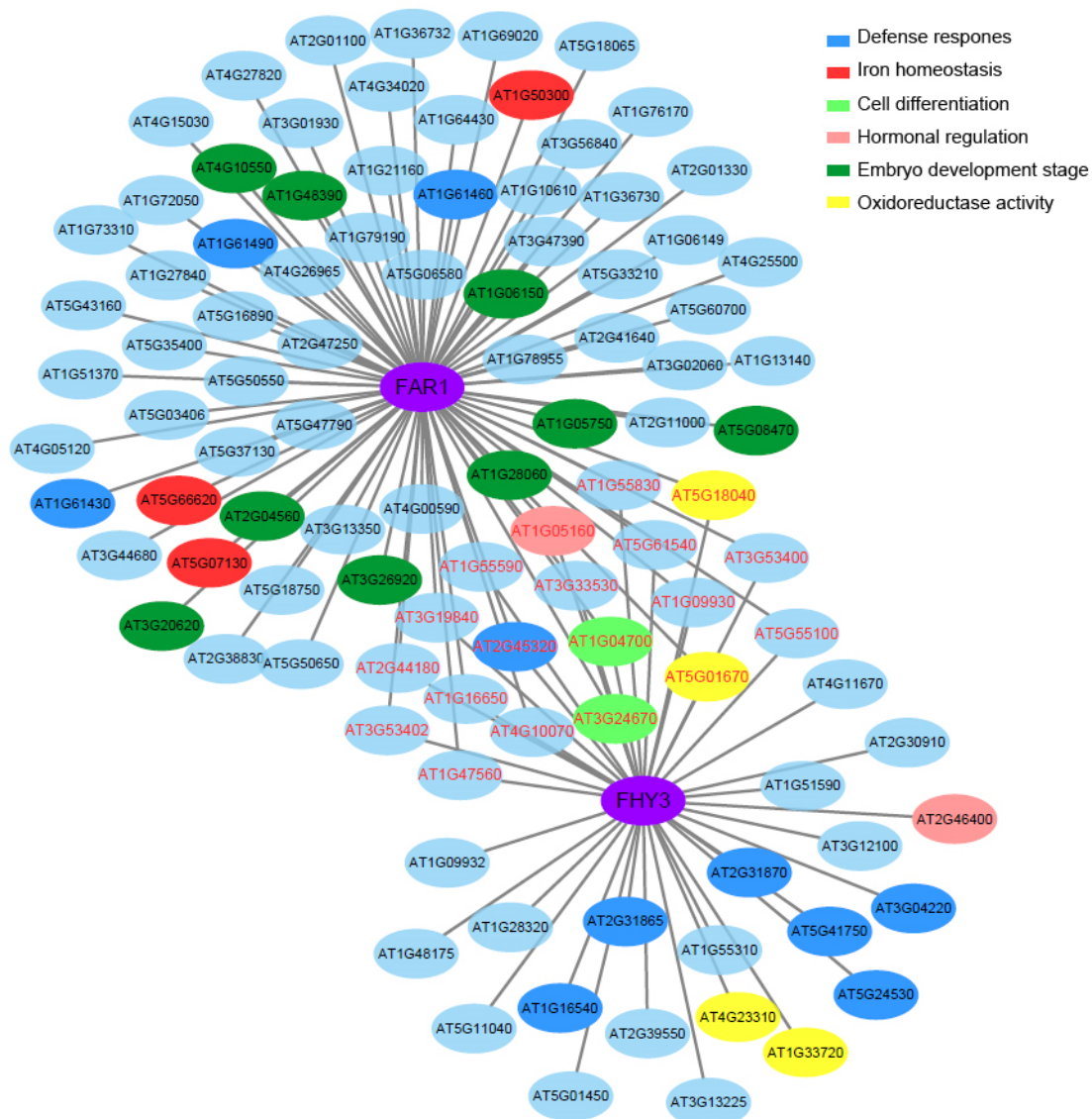
Figure 7 Coexpressed network analysis of FHY3 and FAR1. FHY3/FAR1-coexpression module was created using Cytoscape ver. 3.4.10. Red-labeled genes represent coexpressed genes of both FHY3 and FAR1. Edges with correlation values smaller than 0.9 were removed.

and EDS1-YFP[C] resulted in strong fluorescence in the nuclei of *N. benthamiana* leaves (Figure 8C), suggesting that FAR1 and EDS1 interact in this subcellular compartment. However, expression of either FAR1 or EDS1 failed to produce YFP fluorescence. Thus, we conclude that FAR1 and EDS1 interact in the nucleus.

To explore the molecular relevance of the FAR1-EDS1 interaction, we constructed a luciferase reporter gene driven by *SID2* (*SALICYLIC-ACID-INDUCTION DEFICIENT*, which encodes a key enzyme in pathogen-induced SA biosynthesis) promoter (*SID2p:LUC*) and performed a transient expression assay in *N. benthamiana* leaves with FAR1 and/or EDS1 effectors. FAR1 did not affect the expression of *SID2p:LUC*, whereas EDS1 strongly induced its expression (Figure 8D). Most intriguingly, the coexpression of EDS1 with FAR1 markedly reduced the expression promoted by EDS1 alone (Figure 8D), suggesting that FAR1 inhibits the activity of EDS1 on downstream gene expression. To further investigate the effect of FHY3/FAR1 on the molecular function of EDS1, we comparatively analyzed the gene regulatory function of FHY3/FAR1 and EDS1 on the transcriptome level. Through the analysis of the gene expression profiles of 4-week-old *fhy3 far1* and *eds1*, we found that 142 out of 274 (52%) EDS1-induced genes were represented
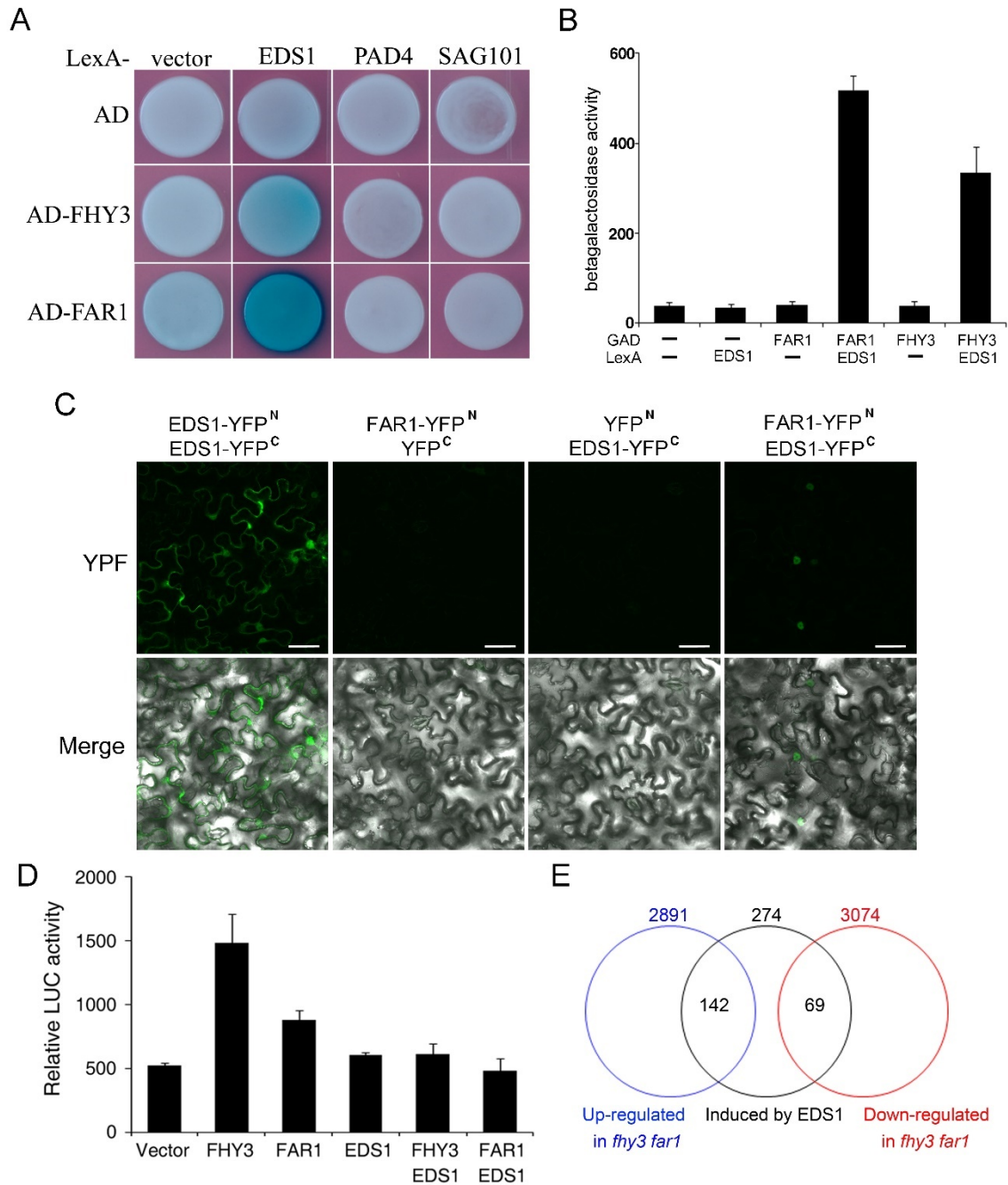
Figure 8 Interaction between FAR1 and EDS1. (**A**) Yeast two-hybrid assay showing the interaction between LexA- and AD-fused proteins. Growth of blue yeast cells indicates an interaction between the two proteins. (**B**) Quantification of yeast two-hybrid interactions by determining β-galactosidase activity. Bars indicate the *SD* of six individual yeast colonies. (**C**) BiFC assay showing that YFP^N-FAR1 and EDS1-YFP^C interact to reconstitute a functional yellow fluorescence protein (YFP) in the nucleus (indicated by arrows) of *Nicotiana benthamiana* leaves. Bar: 50 μm. (**D**) Transient expression assay of *SID2p:LUC* in *N. benthamiana*. Relative LUC activity was normalized to the *35S:GUS* internal control. Bars indicate the *SD* of three replicates. (**E**) Venn diagrams showing the overlap of differentially regulated genes in *fhy3 far1* with previously reported EDS1-induced genes (Bartsch et al., 2006).

in the downregulated group of FHY3/FAR1 while 69 (25%) EDS1-induced genes were found to be downregulated in *fhy3 far1* (Figure 8E) (Bartsch et al., 2006). Together, these results indicate that FHY3 and FAR1 are involved in the defense response, likely through the ESD1-mediated immune signaling pathway.

4. Discussion

4.1. FHY3 and FAR1 Play a Broad Regulatory Role in Plant Phase Growth

As sessile organisms, plants need to adjust themselves in time according to changes in the external environment. The extensive molecular interplay between external and internal signals allows for a plant's developmental regularity. In this study, we revealed three major biological processes during the early 4 weeks of plant growth using a time-course transcriptome analysis: morphogenesis promoted in the second week, large-scale defense responses triggered in the third week, and rapid biomass accumulation supported by increased photosynthesis in the fourth week. RNA-seq analysis revealed that the loss of both FHY3 and FAR1 completely disturbed the three aforementioned biological processes. In the *fhy3 far1* mutant, defense responses were pretriggered in the second week, while morphogenesis-related microtubules activity was delayed to the third week, and photosynthesis was also affected in the fourth week. These indicate that FHY3 and FAR1 play a wide regulatory function on plant growth and development in various developmental stages. Although research on the physiological and molecular mechanisms of FHY3/FAR1 in many biological processes has made great progress, when and how they sense plant endogenous growth signals and integrate various environmental signals to play their growth-dependent regulating functions still require further study.

4.2. FHY3/FAR1 Integrate Plant Immune Signaling

EDS1 and PAD4 localize to both the nucleus and cytosol. The dynamic distribution between these two compartments upon pathogen recognition is likely responsible for proper signal relay (Garcia et al., 2010; Wiermer et al., 2007). Two studies have improved our understanding of defense signaling by revealing that EDS1 forms protein complexes with the TIR-NBS-LRR disease resistance proteins RPS4 and RPS6 in the nuclei and activates defense signaling (Bhattacharjee et al., 2011; Heidrich et al., 2011). However, the nuclear actions of EDS1 remain poorly understood. Our finding that FAR1 interacts with EDS1 and represses its activity sheds light on the molecular role of EDS1 in the nucleus, where it might regulate transcriptional reprograming by interacting with other transcription regulators. In addition, certain photoreceptor mutants (e.g., *phyB*) have shown some susceptible phenotypes (Kazan & Manners, 2011). This indicates that light has a profound influence on plant immunity. Our study links two key components of the phyA signaling pathway, FHY3 and FAR1, with the defense response, and we found that these two factors likely function as a node of crosstalk between light and immune signaling. Further investigation is needed to elucidate the molecular mechanisms behind their effects on the downstream gene expression of EDS1.

5. Supporting Material

The following supporting material is available for this article:

- Figure S1. Enrichment of selected categories of GO biological processes in genes downregulated in the 2, 3, 4-week leaves of NO compared to the previous week.
- Figure S2. Enrichment of selected categories of GO biological processes in genes upregulated in the 2, 3, 4-week leaves of *fhy3 far1* compared to the previous week.
- Figure S3. Enrichment of selected categories of KOG biological processes in genes upregulated in the 2, 3, 4-week leaves of *fhy3 far1* compared to the previous week.
- Table S1. List of primers used in this study.
- Appendix S1. Summary of characteristic genes in the different development stage of wild type (NO) and mutant (*fhy3 far1*).

References

Bartsch, M., Gobbato, E., Bednarek, P., Debey, S., Schultze, J., Bautor, J., & Parker, J. (2006). Salicylic acid-independent ENHANCED DISEASE SUSCEPTIBILITY1 signaling in *Arabidopsis* immunity and cell death is regulated by Monooxygenase *FMO1* and the Nudix Hydrolase *NUD7*. *The Plant Cell*, *18*, 1038–1051. https://doi.org/10.1105/tpc.105.039982

Bhattacharjee, S., Halane, M. K., Kim, S. H., & Gassmann, W. (2011). Pathogen effectors target *Arabidopsis* EDS1 and alter its interactions with immune regulators. *Science*, *334*, 1405–1408. https://doi.org/10.1126/science.1211592

Blasing, O. E., Gibon, Y., Günther, M., Höhne, M., Morcuende, R., Osuna, D., Thimm, O., Usadel, B., Scheible, W. R., & Stitt, M. (2005). Sugars and circadian regulation make major contributions to the global regulation of diurnal gene expression in *Arabidopsis*. *The Plant Cell*, *17*, 3257–3281. https://doi.org/10.1105/tpc.105.035261

Bürstenbinder, K., Rzewuski, G., Wirtz, M., Hell, R., & Sauter, M. (2007). The role of methionine recycling for ethylene synthesis in *Arabidopsis*. *The Plant Journal*, *49*, 238–249. https://doi.org/10.1111/j.1365-313X.2006.02942.x

Cassat, J. E., & Skaar, E. P. (2013). Iron in infection and immunity. *Cell Host & Microbe*, *13*, 509–519. https://doi.org/10.1016/j.chom.2013.04.010

Chen, D., Xu, G., Tang, W., Jing, Y., Ji, Q., Fei, Z., & Lin, R. (2013). Antagonistic basic helix-loop-helix/bZIP transcription factors form transcriptional modules that integrate light and reactive oxygen species signaling in *Arabidopsis*. *The Plant Cell*, *25*, 1657–1673. https://doi.org/10.1105/tpc.112.104869

Clontech. (2009). *Yeast protocols handbook*. https://www.takarabio.com/assets/documents/User%20Manual/PT3024-1.pdf

Colangelo, E. P., & Guerinot, M. L. (2004). The essential basic helix-loop-helix protein FIT1 is required for the iron deficiency response. *The Plant Cell*, *16*, 3400–3412. https://doi.org/10.1105/tpc.104.024315

Considine, M. J., & Foyer, C. H. (2014). Redox regulation of plant development. *Antioxidants & Redox Signaling*, *21*, 1305–1326. https://doi.org/10.1089/ars.2013.5665

Ding, Z. J., Yan, J. Y., Li, C. X., Li, G. X., Wu, Y. R., & Zheng, S. J. (2015). Transcription factor WRKY46 modulates the development of *Arabidopsis* lateral roots in osmotic/salt stress conditions via regulation of ABA signaling and auxin homeostasis. *The Plant Journal*, *84*, 56–69. https://doi.org/10.1111/tpj.12958

Ding, Z. J., Yan, J. Y., Xu, X. Y., Yu, D. Q., Li, G. X., Zhang, S. Q., & Zheng, S. J. (2014). Transcription factor WRKY46 regulates osmotic stress responses and stomatal movement independently in *Arabidopsis*. *The Plant Journal*, *79*, 13–27. https://doi.org/10.1111/tpj.12538

Dossa, K., Mmadi, M. A., Zhou, R., Zhang, T. Y., Su, R. Q., Zhang, Y. J., Wang, L. H., You, J., & Zhang, X. R. (2019). Depicting the core transcriptome modulating multiple abiotic stresses responses in sesame (*Sesamum indicum* L.). *International Journal of Molecular Sciences*, *20*, Article 3930. https://doi.org/10.3390/ijms20163930

Feys, B., Moisan, L., Newman, M., & Parker, J. (2001). Direct interaction between the *Arabidopsis* disease resistance signaling proteins, EDS1 and PAD4. *The EMBO Journal*, *20*, 5400–5411. https://doi.org/10.1093/emboj/20.19.5400

Feys, B., Wiermer, M., Bhat, R., Moisan, L., Medina-Escobar, N., Neu, C., Cabral, A., & Parker, J. (2005). *Arabidopsis* SENESCENCE-ASSOCIATED GENE101 stabilizes and signals within an ENHANCED DISEASE SUSCEPTIBILITY1 complex in plant innate immunity. *The Plant Cell*, *17*, 2601–2613. https://doi.org/10.1105/tpc.105.033910

Ganz, T., & Nemeth, E. (2015). Iron homeostasis in host defence and inflammation. *Nature Reviews Immunology*, *15*, 500–510. https://doi.org/10.1038/nri3863

Garcia, A. V., Blanvillain-Baufume, S., Huibers, R. P., Wiermer, M., Li, G., Gobbato, E., Rietz, S., & Parker, J. E. (2010). Balanced nuclear and cytoplasmic activities of EDS1 are required for a complete plant innate immune response. *PLoS Pathogens*, *6*, Article e1000970. https://doi.org/10.1371/journal.ppat.1000970

Götz, S., García-Gómez, J. M., Terol, J., Williams, T. D., Nagaraj, S. H., Nueda, M. J., Robles, M., Talón, M., Dopazo, J., & Conesa, A. (2008). High-throughput functional annotation and data mining with the Blast2GO suite. *Nucleic Acids Research*, *36*(10), 3420–3435. https://doi.org/10.1093/nar/gkn176

Hamada, T., Takeuchi, N., Kato, T., Fujiwara, M., Sonobe, S., Fukao, Y., & Hashimoto, T. (2013). Purification and characterization of novel microtubule-associated proteins from *Arabidopsis* cell suspension cultures. *Plant Physiology*, *163*, 1804–1816. https://doi.org/10.1104/pp.113.225607

Heidrich, K., Wirthmueller, L., Tasset, C., Pouzet, C., Deslandes, L., & Parker, J. E. (2011). *Arabidopsis* EDS1 connects pathogen effector recognition to cell compartment-specific immune responses. *Science*, *334*, 1401–1404. https://doi.org/10.1126/science.1211641

Hu, Y., Dong, Q., & Yu, D. (2012). *Arabidopsis* WRKY46 coordinates with WRKY70 and WRKY53 in basal resistance against pathogen *Pseudomonas syringae*. *Plant Science*, *185–186*, 288–297. https://doi.org/10.1016/j.plantsci.2011.12.003

Hudson, M., Ringli, C., Boylan, M. T., & Quail, P. H. (1999). The *FAR1* locus encodes a novel nuclear protein specific to phytochrome A signaling. *Genes & Development*, *13*, 2017–2027. https://doi.org/10.1101/gad.13.15.2017

Jakoby, M., Wang, H. Y., Reidt, W., Weisshaar, B., & Bauer, P. (2004). *FRU (BHLH029)* is required for induction of iron mobilization genes in *Arabidopsis thaliana*. *FEBS Letters*, *577*, 528–534. https://doi.org/10.1016/j.febslet.2004.10.062

Kazan, K., & Manners, J. M. (2011). The interplay between light and jasmonate signaling during defense and development. *Journal of Experimental Botany*, *62*, 4087–4100. https://doi.org/10.1093/jxb/err142

Li, G., Siddiqui, H., Teng, Y., Lin, R., Wan, X. Y., Li, J., Lau, O. S., Ouyang, X., Dai, M., Wan, J., Devlim, P. F., Deng, X. W., & Wang, H. (2011). Coordinated transcriptional regulation underlying the circadian clock in *Arabidopsis*. *Nature Cell Biology*, *13*, 616–622. https://doi.org/10.1038/ncb2219

Liang, H., Zhang, Y., Martinez, P., Rasmussen, C. G., Xu, T. D., & Yang, Z. B. (2018). The microtubule-associated protein IQ67 DOMAIN5 modulates microtubule dynamics and pavement cell shape. *Plant Physiology*, *177*, 1555–1568. https://doi.org/10.1104/pp.18.00558

Lin, R., Ding, L., Casola, C., Ripoll, D. R., Feschotte, C., & Wang, H. (2007). Transposase-derived transcription factors regulate light signaling in *Arabidopsis*. *Science*, *318*, 1302–1305. https://doi.org/10.1126/science.1146281

Lloyd, C., & Hussey, P. (2001). Microtubule-associated proteins in plants-why we need a MAP. *Nature Reviews Molecular Cell Biology*, *2*, 40–47. https://doi.org/10.1038/35048005

Luo, Y., Han, Z., Chin, S. M., & Linn, S. (1994). Three chemically distinct types of oxidants formed by ironmediated Fenton reactions in the presence of DNA. *Proceedings of the National Academy of Sciences of the United States of America* (Vol. 91, pp. 12438–12442). https://doi.org/10.1073/pnas.91.26.12438

Ma, L., Tian, T., Lin, R., Deng, X. W., Wang, H., & Li, G. (2016). *Arabidopsis* FHY3 and FAR1 regulate light-induced *myo*-inositol biosynthesis and oxidative stress responses by transcriptional activation of *MIPS1*. *Molecular Plant*, *9*(4), 541–557. https://doi.org/10.1016/j.molp.2015.12.013

Mittler, R., Vanderauwera, S., Suzuki, N., Miller, G., Tognetti, V. B., Vandepoele, K., Gollery, M., Shulaev, V., & Breusegem, F. (2011). ROS signaling: The new wave? *Trends in Plant Science*, *16*, 300–309. https://doi.org/10.1016/j.tplants.2011.03.007

Nagano, A. J., Tetsuhiro, K., Sugisaka, J., Honjo, M. N., Iwayama, K., & Kudoh, H. (2019). Annual transcriptome dynamics in natural environments reveals plant seasonal adaptation. *Nature Plants*, *5*, 74–83. https://doi.org/10.1038/s41477-018-0338-z

Neff, M. M., Fankhauser, C., & Chory, J. (2000). Light: An indicator of time and place. *Genes & Development*, *14*, 257–271. https://doi.org/10.1101/gad.14.3.257

Ouyang, X., Li, J., Li, G., Li, B., Chen, B., Shen, H., Huang, X., Mo, X., Wan, X., Lin, R., Li, S., Wang, H., & Deng, X. W. (2011). Genome-wide binding site analysis of FAR-RED ELONGATED HYPOCOTYL3 reveals its novel function in *Arabidopsis* development. *The Plant Cell*, *23*, 2514–2535. https://doi.org/10.1105/tpc.111.085126

Sasabe, M., Soyano, T., Takahashi, Y., Sonobe, S., Igarashi, H., Itoh, T., Hidaka, M., & Machida, Y. (2006). Phosphorylation of NtMAP65-1 by a MAP kinase down-regulates its activity of MT bundling and stimulates progression of cytokinesis of tobacco cells. *Genes & Development*, *20*, 1004–1014. https://doi.org/10.1101/gad.1408106

Schiessl, K., Muino, J. M., & Sablowski, R. (2014). *Arabidopsis* JAGGED links floral organ patterning to tissue growth by repressing Kip-related cell cycle inhibitors. *Proceedings of the National Academy of Sciences of the United States of America* (Vol. 111, pp. 2830–2835). https://doi.org/10.1073/pnas.1320457111

Sedbrook, J. C. (2004). MAPs in plant cells: Delineating microtubule growth dynamics and organization. *Current Opinion in Plant Biology*, *7*, 632–640. https://doi.org/10.1016/j.pbi.2004.09.017

Singh, M., Gupta, A., Singh, D., Khurana, J. P., & Laxmi, A. (2017). *Arabidopsis* RSS1 mediates cross-talk between glucose and light signaling during hypocotyl elongation growth. *Scientific Reports*, *7*, Article 16101. https://doi.org/10.1038/s41598-017-16239-y

Smoot, M., Ono, K., Ideker, T., & Maere, S. (2011). PiNGO: A Cytoscape plugin to find candidate genes in biological networks. *Bioinformatics*, *27*, 1030–1031. https://doi.org/10.1093/bioinformatics/btr045

Tang, W., Ji, Q., Huang, Y., Jiang, Z., Bao, M., Wang, H., & Lin, R. (2013). FAR-RED ELONGATED HYPOCOTYL3 and FAR-RED IMPAIRED RESPONSE1 transcription factors integrate light and abscisic acid signaling in *Arabidopsis*. *Plant Physiology*, *163*, 857–866. https://doi.org/10.1104/pp.113.224386

Tang, W., Wang, W., Chen, D., Ji, Q., Jing, Y., Wang, H., & Lin, R. (2012). Transposase-derived proteins FHY3/FAR1 interact with PHYTOCHROME-INTERACTING FACTOR1 to regulate chlorophyll biosynthesis by modulating *HEMB1* during deetiolation in *Arabidopsis*. *The Plant Cell*, *4*, 1984–2000. https://doi.org/10.1105/tpc.112.097022

Vlot, A., Dempsey, D., & Klessig, D. (2009). Salicylic acid, a multifaceted hormone to combat disease. *Annual Review of Phytopathology*, *47*, 177–206. https://doi.org/10.1146/annurev.phyto.050908.135202

Voinnet, O., Rivas, S., Mestre, P., & Baulcombe, D. (2003). An enhanced transient expression system in plants based on suppression of gene silencing by the p19 protein of tomato bushy stunt virus. *The Plant Journal*, *33*, 949–956. https://doi.org/10.1046/j.1365-313X.2003.01676.x

Walter, M., Chaban, C., Schutze, K., Batistic, O., Weckermann, K., Nake, C., Blazevic, D., Grefen, C., Schumacher, K., Oecking, C., Harter, K., & Kudla, J. (2004). Visualization of protein interactions in living plant cells using bimolecular fluorescence complementation. *The Plant Journal*, *40*, 428–438. https://doi.org/10.1111/j.1365-313X.2004.02219.x

Wang, H., & Deng, X. W. (2002). *Arabidopsis* FHY3 defines a key phytochrome A signaling component directly interacting with its homologous partner FAR1. *The EMBO Journal*, *21*, 1339–1349. https://doi.org/10.1093/emboj/21.6.1339

Wang, W., Tang, W., Ma, T., Niu, D., Jin, J. B., Wang, H., & Lin, R. (2016). A pair of light signaling factors FHY3 and FAR1 regulates plant immunity by modulating chlorophyll biosynthesis. *Journal of Integrative Plant Biology*, *58*, 91–103. https://doi.org/10.1111/jipb.12369

Wasteneys, G., & Ambrose, J. (2009). Spatial organization of plant cortical microtubules: Close encounters of the 2D kind. *Trends in Cell Biology*, *19*, 62–71. https://doi.org/10.1016/j.tcb.2008.11.004

Whitelam, G. C., Johnson, E., Peng, J., Carol, P., Anderson, M. L., Cowl, J. S., & NP.1993, H. (1993). Phytochrome A null mutants of *Arabidopsis* display a wild-type phenotype in white light. *The Plant Cell*, *5*, 757–768. https://doi.org/10.1105/tpc.5.7.757

Wiermer, M., Palma, K., Zhang, Y., & Li, X. (2007). Should I stay or should I go? Nucleocytoplasmic trafficking in plant innate immunity. *Cellular Microbiology*, *9*, 1880–1890. https://doi.org/10.1111/j.1462-5822.2007.00962.x

Willems, P., Mhamdi, A., Stael, S., Storme, V., Kerchev, P., Noctor, G., Gevaert, K., & Van, B. (2016). The ROS Wheel: Refining ROS transcriptional footprints in *Arabidopsis*. *Plant Physiology*, *171*, 1720–1733. https://doi.org/10.1104/pp.16.00420

Yamamoto, Y. Y., Matsui, M., Ang, L. H., & Deng, X. W. (1998). Role of a COP1 interactive protein in mediating light-regulated gene expression in *Arabidopsis*. *The Plant Cell*, *10*, 1083–1094. https://doi.org/10.1105/tpc.10.7.1083

Yi, F., Gu, W., Chen, J., Song, N., Gao, X., Zhang, X. B., Zhou, Y. S., Ma, S., WB, Z., HM, E., E, P., A, P., NJ, L., & J. (2019). *High temporal-resolution transcriptome landscape of early maize seed development* (Vol. 31). https://doi.org/10.1105/tpc.18.00961